

NSG-135
U Hawaii

F-REGION NIGHTGLOW EMISSIONS OF ATOMIC OXYGEN

II. ANALYSIS OF 6300Å AND ELECTRON DENSITY DATA*

by

Vern L. Peterson
Environmental Science Services Administration
Institute for Telecommunication Sciences and Aeronomy**
Boulder, Colorado

and

Walter R. Steiger
Hawaii Institute of Geophysics, University of Hawaii

N66-19093

FACILITY FORM 602

(ACCESSION NUMBER)	(THRU)
33	1
(PAGES)	(CODE)
CR 70853	13
(NASA CR OR TMX OR AD NUMBER)	(CATEGORY)

GPO PRICE \$

CFSTI PRICE(S) \$

Hard copy (HC) \$200

Microfiche (MF) 50

ff 653 July 65

*Hawaii Institute of Geophysics Contribution No. 127

**Formerly the Central Radio Propagation Laboratory,
National Bureau of Standards

F-Region Nightglow Emissions of Atomic Oxygen

II. Analysis of 6300Å and Electron Density Data

by

Vern L. Peterson
Environmental Science Services Administration
Institute for Telecommunication Sciences and Aeronomy
Boulder, Colorado

and

Walter R. Steiger
Hawaii Institute of Geophysics, University of Hawaii

ABSTRACT

19093

Nightglow 6300Å and electron density data from Maui, Hawaii have been analyzed by using the formulas of Paper I. The observed 6300Å emission is found to consist of two components. The primary component may vary considerably during the night and its variations are explained satisfactorily by the chemical reactions discussed in Paper I; these variations correspond to variations in the height, shape, and magnitude of the electron density profile. The secondary, or background, component does not seem to vary rapidly during the night but may vary considerably from one night to another. The source of the background component is unknown. It is shown that the magnitude deduced for it is insensitive to errors in the many parameters that enter the calculations. Finally, even though the theory given in Paper I does satisfactorily explain the observations, the pertinent chemical reactions seem to be inefficient in producing the 6300Å nightglow.

autho

KEY WORDS: 6300Å nightglow - electron density profiles - Maui, Hawaii
data - dissociative recombination - data analysis -
background component

INTRODUCTION

Dissociative recombination in the F region appears to be the dominant process, at night and at low latitudes, for producing the excited oxygen atoms that give rise to the 6300\AA nightglow. The theory based on this mechanism, relating ionospheric parameters to the 6300\AA nightglow intensity, has been investigated by various authors [Chamberlain, 1958; Barbier, 1959; Lagos, Bellew, and Silverman, 1963]. A detailed version of this theory is given in Paper I [Peterson, VanZandt, and Norton, 1965]. The purpose of the present paper is to give the results of an analysis of electron density and 6300\AA intensity data using the formulas given in Paper I. Below, we will show that the observed variations in 6300\AA are satisfactorily explained as being caused by corresponding variations in the ionosphere; the data also show the presence of a background component which is not explained by the theory. The component of the 6300\AA nightglow that is explained by the theory shows that the chemical reactions discussed in Paper I have a low efficiency in producing $\text{O}(^1\text{D})$.

SELECTION OF DATA

Ionospheric observations have been made on a routine basis from Maui, Hawaii (21°N , 156°W geographic; 21°N , 88°W geomagnetic; 22°N dip latitude; 39° dip angle) for several years. Since July 1961, photometric observations have also been routinely made. The ionospheric soundings are made once every 15 minutes (day and night) and the airglow observations at 6300\AA are made (at night) once every five minutes with a zenith photometer and once every 15 minutes with an all-sky scanning photometer. The present study used the zenith photometer data (see Purdy, et al., 1961 for a

description of the instrumentation); the zenith data from the all-sky scanning photometer are essentially the same, however.

For the present study simultaneous ionospheric and photometric observations were needed. This limits the amount of data usable. Since nightglow measurements are made only under the best of observing conditions, observations are limited to the two weeks centered around new moon and to times free from clouds or haze. Also, in order to facilitate comparison with theory, the data are further restricted to cases in which a variation of at least 20 Rayleighs is observed during the period of observation.

Even though ionosonde measurements are made nearly every night, only a small percentage of the ionograms yield good electron density profiles, $n(h)$. Any method used to reduce nighttime ionograms to $n(h)$ profiles is extremely sensitive to the data available at the low frequency end of the ionogram. Sporadic E ionization and radio interference (noise), which are quite common for Maui, often cause the low frequency echoes from the F region to be lost.

The nighttime ionograms that yield the most reliable $n(h)$ profiles are those that actually show echoes from the normal E layer or from the so-called intermediate layer; the ionograms that yield slightly less reliable $n(h)$ profiles are those that do not actually show E-region echoes but do show retardation on the low frequency end of the F-region echoes, indicating that low-lying ionization is present; and finally, the ionograms that yield $n(h)$ profiles of only marginal quality are those that show neither E-region echoes nor low frequency retardation of the F-region echoes. In the following discussion, the $n(h)$ profiles from the above three types of ionograms will be referred to as being of quality 1, 2,

or 3, respectively.

The amount of simultaneous data finally selected depends upon the quality desired and upon the objective of the data analysis. Unfortunately, nighttime quality 1 ionograms are so scarce that no long sequence could be found. Since one of the objectives of the data analysis was to follow the variations of the "linear recombination coefficient" during a night, a long sequence was needed. Consequently, some lower quality $n(h)$ data had to be used. The data used consist of two short sequences of quality 1 data, and a few long sequences of quality 2 and 3 data, as listed in table 1.

In this study, $n(h)$ profiles were calculated by the method of Paul [Paul and Wright, 1963], and full corrections were attempted for the effects of ionization underlying the F region.

Observed and Calculated 6300Å Nightglow Intensities (in Rayleighs)

5

TABLE 1 (continued)

Observed and Calculated 6300A Nightglow Intensities (in Rayleighs)									
Quality 1		Quality 2		Quality 3					
Sept. 17/18, 1961		Apr. 1/2, 1962		Oct. 29/30, 1962		Feb. 23/24, 1963		Feb. 24/25, 1963	
L T	Q(obs) Q(calc)*	Q(obs) Q(calc)*	Q(obs) Q(calc)*	Q obs	Q(calc)*	Q(obs)	Q(calc)*	Q(obs)	Q(calc)*
0215				60	16	51	16	35	11
30				56	16	50	16	34	14
45				67	19	44	17	43	24
0300				62	14	48	18	57	32
15	(95)** 33	(57)	44	51	12	48	22	62	35
30	90 25	57	45	46	9	43	20	59	30
45	76 25	44	39	45	7	38	18	47	26
0400	78 14	43	37	49	5	30	12	44	24
15	67 10	37	22	46	4	(33)	12	(35)	17
30		30	19	41	4	(31)	11	26	15
45		32	14	41	5	29	12	33	13
0500			12	42	6	31	10	29	14

The $Q(\text{calc})$ shown here are for $k_{D2} = 0$, $k_{D1}^ X(300) = 0.1$, $\alpha_2(00) = 10^{-7} \text{ cm}^3 \text{ sec}^{-1}$ and $\beta_2(300) = 10^{-4} \text{ sec}^{-1}$, which may or may not be appropriate for any particular time; see text.

**** $Q(\text{obs})$ values in parentheses have been extrapolated by 5 minutes.**

ANALYSIS OF DATA

That portion of the 6300Å nightglow that arises from chemical reactions in the F region was shown in Paper I to have a zenith intensity of Q_{6300} (Rayleighs) =

$$0.076 \int_{120}^{500} \frac{K(h)}{1 + d_D(h)/.0091} \cdot \frac{\beta_2(h) n(h)}{1 + [1 + X(h)/3X(200)] \beta_2(h)/\alpha_2(h)n(h)} dh \quad (1)$$

where

$$X(h) = \beta_1(h)/\beta_2(h) = X(300) \exp(-z_{28}(h)/7),$$

$$\beta_2(h) = \beta_2(300) \frac{T(300)}{T(h)} \exp(-z_{28}(h)),$$

and

$$K(h) = k_{D2} + k_{D1}^* X(h) = k_D(h) X(h), \quad k_{D1}^* = k_{D1} + .94 k_{S1}.$$

The α 's are the specific reaction rates for dissociative recombination, the β 's are the linear recombination coefficients, the k 's are the number of excitations per recombination and may be thought of as "efficiencies" of the chemical reactions in producing $O(^1D)$ and $O(^1S)$, z is the reduced height, n is electron density, and d_D is the collisional deactivation coefficient. The subscript notation is: except for z , 1 refers to reactions involving O_2^+ , 2 refers to reactions involving NO^+ , and D and S refer to the 1D and 1S levels of oxygen; for z , the subscript is the molar weight of the atom or molecule referred to, so that 28 refers to N_2 .

Note that equation (1) includes the contributions to Q_{6300} from both the O_2^+ and NO^+ reactions, as discussed in Paper I. To simplify the numerical work β_1 and α_1 should be put on terms of β_2 and α_2 , or vice versa. As can be seen, equation (1) and the following discussion have been cast in terms of β_2 and α_2 . This

choice was made, and the calculations performed, prior to the publishing of the paper by Dalgarno and Walker [1964] which pointed out that the NO^+ reactions will not produce much $\text{O}(^1\text{D})$ excitation. The computations could be repeated in terms of β_1 and α_1 , and this would change some of the numbers reported here. However, the conclusions of this paper would not be changed and so it is felt that such recalculations are unnecessary.

As mentioned in Paper I, the α 's are thought to have a $T^{-1 \pm \frac{1}{2}}$ dependence. For purposes of numerical evaluation, α_2 was assumed to vary as T^{-1} :

$$\alpha_2(h) = \alpha_2(300) T(300)/T(h).$$

The F region is nearly isothermal, however, and so an error in this choice has a negligible effect on the final results. In equation (1), the constant term before the integral includes the appropriate conversion factors to allow height to be expressed in kilometers and the nightglow intensity in Rayleighs; also, the limits on the integral have been taken as 120 and 500 km since only a negligible amount of radiation comes from heights beyond these limits. Finally, in the bracketed term $\alpha_2 \beta_1 / \alpha_1 \beta_2$ has been set equal to $X(h)/3X(200)$ since the rocket observations of Johnson, et al. [1958], Taylor and Brinton [1961], and Holmes, et al. [1965] indicate that at 200 km, $\alpha_2 \beta_1 / \alpha_1 \beta_2 \approx 1/3$. An error in this choice has little effect on the final results.

In order to evaluate equation (1) and compare the results with nightglow observations, $n(h)$, $T(h)$, $d_D(h)$ profiles had to be used as data. From an ionogram, only that portion of the $n(h)$ profile up to the F-region peak can be calculated. Since the entire profile is needed, an α - Chapman topside of constant scale-height gradient was added, using for a scale

height at the F-region peak that which is deduced by fitting a parabola to the $n(h)$ bottomside profile at the peak. The $T(h)$ profile was taken from an atmospheric model of Harris and Priester [1962] for the appropriate time of night. And finally, the $d_D(h)$ profile was calculated using $d_D = s_D [O_2]$ with $s_D = 2 \times 10^{-11} \text{ cm}^3 \text{ sec}^{-1}$ and the 2300 model atmosphere of Harris and Priester.

As stated in Paper I, the dependence of Q_{6300} on $\beta_2(300)$ is very strong (nearly linear) whereas the dependence on $\alpha_2(300)$ is very weak. As an example, if we take $\alpha_2(300) = 10^{-7} \text{ cm}^3 \text{ sec}^{-1}$ and increase $\beta_2(300)$ from 10^{-5} to 10^{-4} sec^{-1} for the September 17/18, 1961, 0330 case, Q_{6300} increases by a factor of 8. On the other hand, if we take $\beta_2(300) = 10^{-4} \text{ sec}^{-1}$ and increase $\alpha_2(300)$ from 10^{-8} to $10^{-7} \text{ cm}^3 \text{ sec}^{-1}$ for the same case, Q_{6300} increases by only a factor of 1.6. The dependence of Q_{6300} on $X(300)$ is even stronger than its dependence on $\beta_2(300)$, and for purposes of numerical work the Q_{6300} vs $X(300)$ relation may be considered to be strictly linear. Finally, the dependence of Q_{6300} on k_{D2} and k_{D1}^* is, of course, strictly linear.

A graphical comparison of the theoretical intensities calculated from the $n(h)$ profiles, $Q(\text{calc})$, with the observed intensities, $Q(\text{obs})$, allows us to evaluate the completeness of the theory given in Paper I. Figures 1a and 1b illustrate this comparison for the quality 1 and 2 data listed in table 1, for $k_{D2} = 0$, $k_{D1}^* X(300) = 0.1$, $\alpha_2(300) = 10^{-7} \text{ cm}^3 \text{ sec}^{-1}$, and $\beta_2(300) = 10^{-4} \text{ sec}^{-1}$; the values of k_{D2} , $k_{D1}^*(300)$, etc., used here are immaterial for purposes of testing the completeness of the theory. The slopes of the "least square" lines shown in figures 1a and 1b depend, of course, on the choice of these parameters. In fact, the requirement that

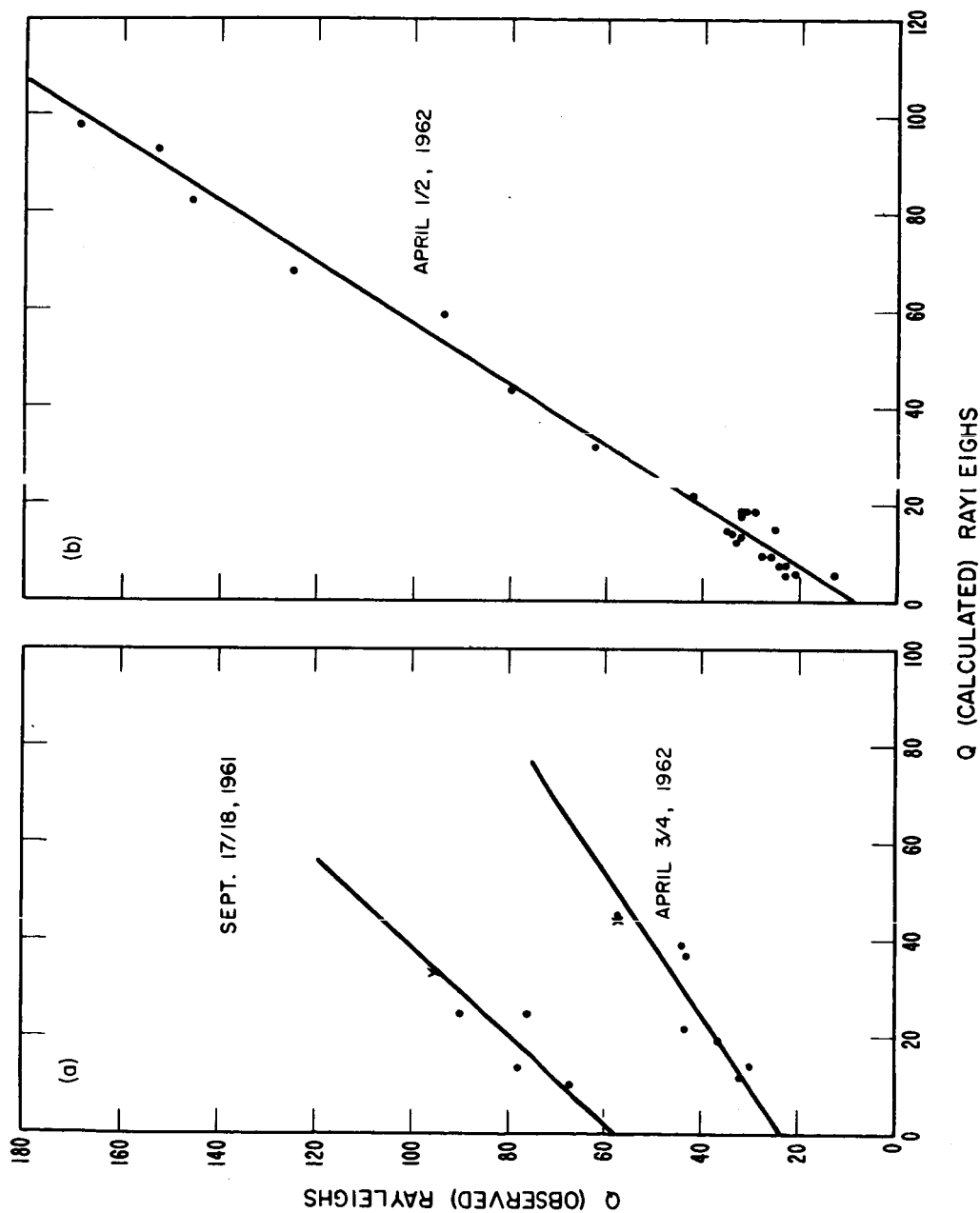


Figure 1. Comparison of the calculated and observed 6300Å nightglow intensities for (a) quality 1 and (b) quality 2 data. The two points marked by crosses in (a) are for $Q(\text{obs})$ extrapolated by five minutes. The intercepts at $Q(\text{calc}) = 0$ represent the amount of background radiation that cannot be explained by the theory given in Paper I. The $Q(\text{calc})$ values are for $k_{D2} = 0$, $k_{D1} \times (300) = 0.1$, $\alpha_0(300) = 1$, $\text{cm}^3 \text{sec}^{-1}$, $\beta_2(300) = 10^{-4} \text{sec}^{-1}$.

the lines should have a slope of 45° determines the values of $K(300)\beta_2(300)$, as discussed below:

If we assume that a "background" component is present for each set of observations, then the agreement between $Q(\text{calc})$ and $Q(\text{obs})$ is good. The value of this background component, $Q(\text{back})$, is easily obtained by extrapolating the set of points back to $Q(\text{calc}) = 0$ (which corresponds to no ionosphere), as indicated in the figure. The fact that the points for a given set cluster fairly closely about a straight line indicates that neither the background component nor the ionospheric parameters $\beta_2(300)$ and $X(300)$ varied significantly during the period of observation. The β ratio, $X(300)$, would not be expected to vary much during the night, but $\beta_2(300)$ and $Q(\text{back})$ might do so. It is conceivable that a variation in $\beta_2(300)$ is just balanced by a variation in $Q(\text{back})$, but this seems unlikely.

A similar comparison of $Q(\text{calc})$ with $Q(\text{obs})$ for the quality 3 data of table 1 does not yield as good a correlation, as shown in figures 2a, 2b, and 2c. Part of the scatter in the points is undoubtedly due to the uncertainty in the $n(h)$ profiles but it seems probable that part of it is real. This can be seen more clearly when it is noticed that observations covering a few hours often cluster about a straight line. In figure 2c, if we choose only those consecutive points that do fall along a line, we can break the night into two groups, each group defining a different (least square) line. The upper line in figure 2c defines the trend for the period 2300-0215 and the lower line the trend for period 0230-0500. This figure cannot be used as evidence that $Q(\text{back})$ changed during the night, however, since the two intercepts can be varied merely

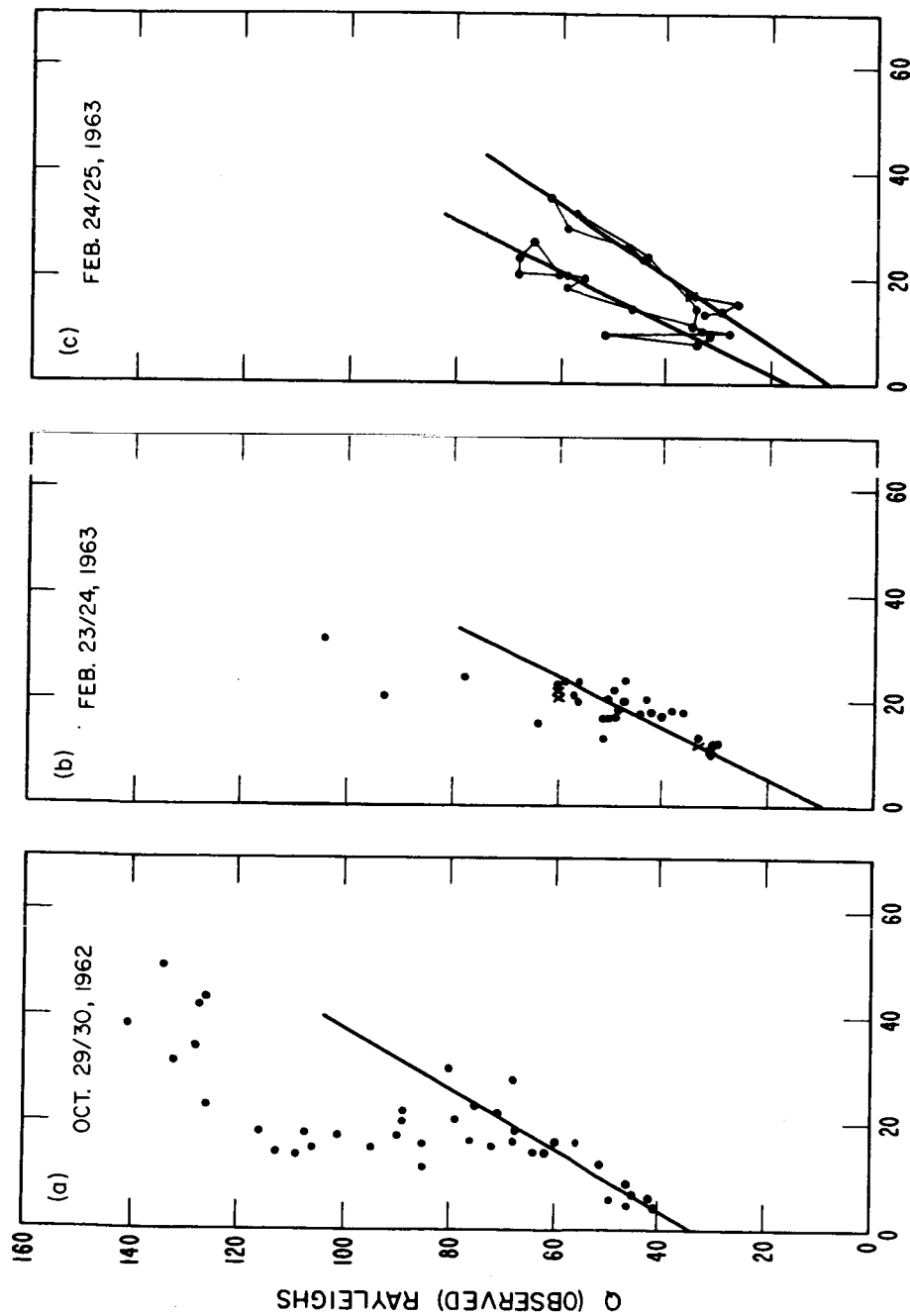


Figure 2. Comparison of the calculated and observed 300Å nightglow intensities for quality 3 data. In (a) and (b), the lines are least square fits for the LT>0000 and LT>2100 data, respectively. In (c), the upper heavy line represents the (least square) correlation during the early part of the observation period (2300-0215), and the lower heavy line that for the latter part (0230-0500); the light lines connect consecutive points. The $Q(\text{calc})$ values are for $k_{D2} = 0$, $k_{D1} \times X(300) = 0.1$, $\alpha_2(300) = 10^{-7} \text{ cm}^3 \text{ sec}^{-1}$, and $\beta_2(300) = 10^{-4} \text{ sec}^{-1}$. As in figure 1, the points marked by crosses represent a five minute extrapolation in $Q(\text{obs})$.

by grouping the points differently.

Figures 2a and 2b cannot be interpreted unambiguously. For example, $\beta_2(300)$ could have been varying in the early part of the night (this is the view pursued below), $Q(\text{back})$ could have been varying, or the theory given in Paper I could have been inadequate for these times. The least square lines shown represent only the latter part of the night: 0000 hours and after for figure 2a and 2100 hours and after for figure 2b.

The source of the background component is not known. At least part of it is contamination by extraneous light (see next section) but the possibility of its reality cannot be discounted. The most likely sources of $Q(\text{back})$ seem to be excitation by impact of high energy particles and excitation by the reaction $N(^2D) + O(^3P) \rightarrow N(^4S) + O(^1D)$. The source of the $N(^2D)$ would supposedly be $NO^+ + e \rightarrow N(^2D) + O(^3P)$.

The numerical value of $Q(\text{back})$ for a given night is very insensitive to the choice of parameters. This is well illustrated by the data of September 17/18, 1961. Figures 3a and 3b show the effect of varying the parameters $\beta_2(300)$ and $\alpha_2(300)$, one at a time. As can be seen, the slope of the least square line is sensitive to the choice of parameters but the intercept, $Q(\text{back})$, is not. This conclusion also applies to variations in k_{D2} and $k_{D1}^* X(300)$, since these parameters are linearly related to Q .

Because $Q(\text{back})$ can be determined fairly precisely for the quality 1 and 2 data, and reasonably estimated for the quality 3 data, it can be subtracted from $Q(\text{obs})$ to leave that portion of the nightglow that is explained by the theory presented in Paper I. The combinations of k_{D2} , $k_{D1}^* X(300)$, $\beta_2(300)$, and $\alpha_2(300)$ which cause $Q(\text{calc})$ to equal $Q(\text{obs}) - Q(\text{back})$ can then be used to investigate the behavior of these parameters.

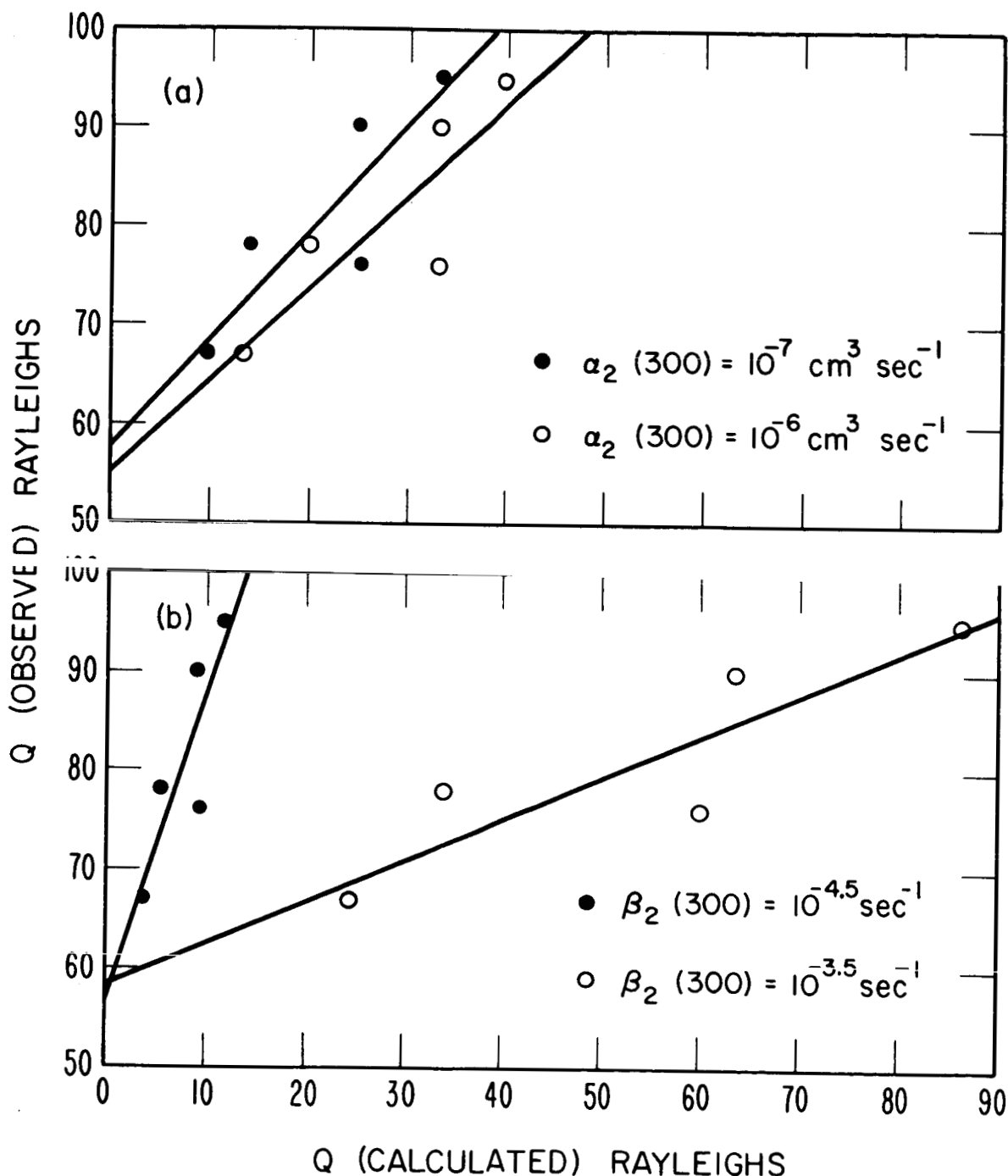


Figure 3. Comparison of the calculated and observed 6300Å nightglow intensities for Sept. 17/18, 1961, showing the effects of varying $\alpha_2(300)$ and $\beta_2(300)$. In both (a) and (b) the calculations were made for $k_{D2} = 0$ and $k_{DL} X(300) = 0.1$. In (a), $\beta_2(300) = 10^{-4} \text{ sec}^{-1}$ and $\alpha_2(300)$ is allowed to assume two different values. The slopes of the lines differ slightly in the two cases, and the background components differ by less than 3 Rayleighs. In (b), $\alpha_2 = 10^{-7} \text{ cm}^3 \text{ sec}^{-1}$ and $\beta_2(300)$ is allowed to assume two different values. The slopes of the two lines differ greatly in the two cases, but the background components differ by less than 2 Rayleighs.

Table 2 lists the values of $Q(\text{back})$ used in the following discussion as well as the range within which $Q(\text{back})$ probably falls.

Figures 4 and 5 illustrate the relation between the various parameters for 2100, April 1, 1962. In both figures, $\beta_2(300)$ is plotted against $k_{D1}^* X(300)$; in figure 4, the curves are parametric in $\alpha_2(300)$ with $k_{D2} = 0$, and in figure 5, the curves are parametric in k_{D2} with $\alpha_2(300) = 10^{-7} \text{ cm}^3 \text{ sec}^{-1}$. (In figures 4 and 5, note that if $k_{D1}^* X(300)$, $\beta_2(300)$, and k_{D2} were replaced by k_{D1}^* , $\beta_1(300)$, and $k_{D2}/X(300)$, respectively, exactly the same curves would be obtained.) Two things may be noticed from these curves or from equation (1). First, since the coefficient $\alpha_2(300)$ is near $10^{-7} \text{ cm}^3 \text{ sec}^{-1}$, even an order of magnitude error in its estimate produces a rather small change in the curve. We can therefore confine our attention to evaluating the other coefficients assuming that $\alpha_2(300) = 10^{-7} \text{ cm}^3 \text{ sec}^{-1}$, knowing that the probable errors produced by this choice are relatively insignificant. Second, the product $K(300) \beta_2(300)$ is nearly independent of $K(300)$ and $\beta_2(300)$ individually; in this case the product is about 10^{-5} sec^{-1} . From only the data examined here it is impossible to evaluate $K(300)$ and $\beta_2(300)$ separately.

TABLE 2

Date	$Q(\text{back})$ (Rayleighs)	
	Used	Range
Sept. 17/18, 1961	57	55-60
April 3/4, 1962	22	20-25
April 1/2, 1962	9	7-12
October 29/30, 1962	32	25-45
February 23/24, 1963	0	0-15
February 24/25, 1963	11	5-20

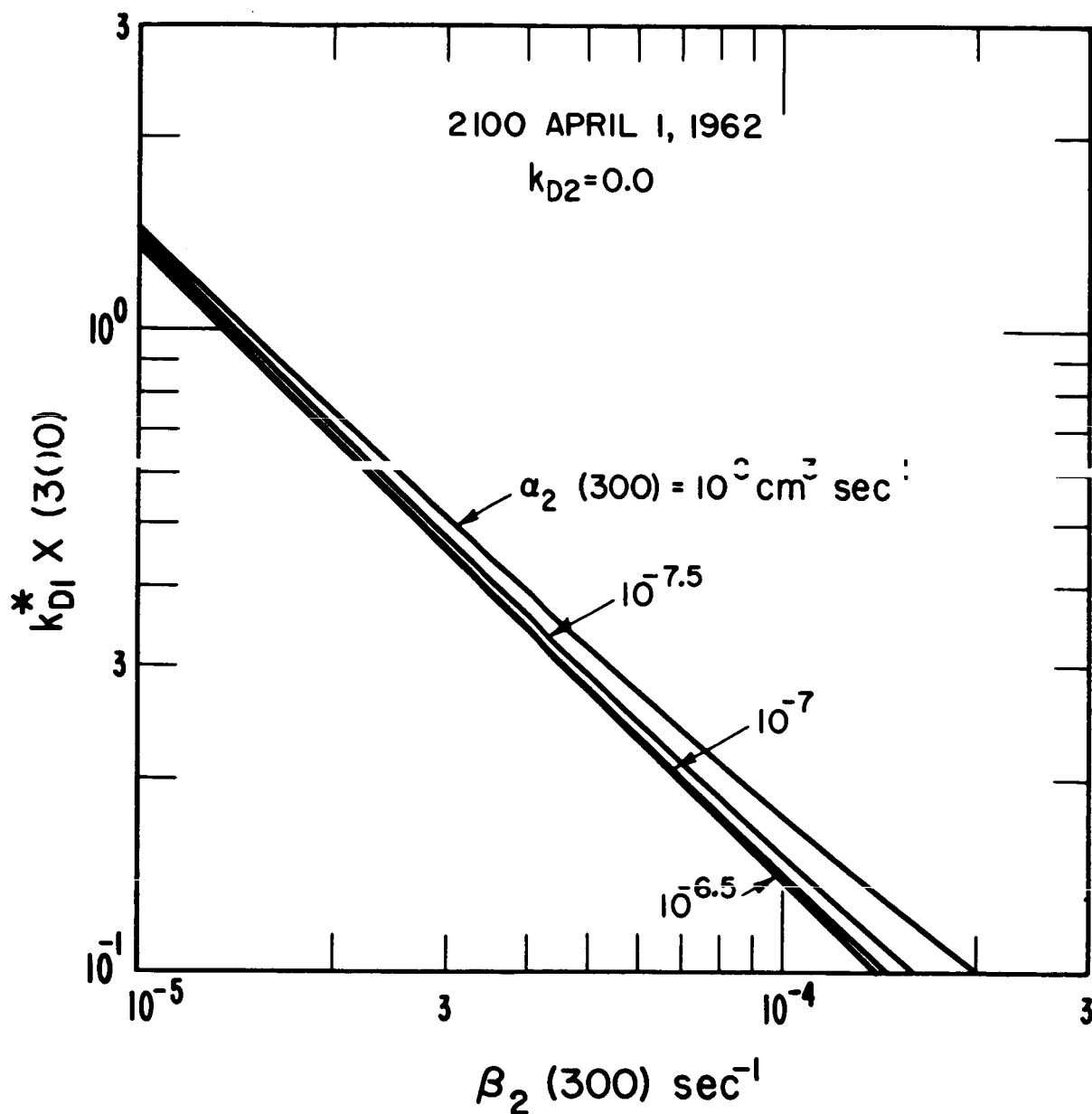


Figure 4. Combinations of $\alpha_2(300)$, $\beta_2(300)$, and $k_{D1}^* X(300)$, for $k_{D2} = 0$, which give $Q(\text{calc}) = Q(\text{obs}) - Q(\text{back})$ for 2100 April 1, 1962. Note that the dependence on $\alpha_2(300)$ is weak for $\alpha_2(300) \approx 10^{-7} \text{ cm}^3 \text{ sec}^{-1}$.

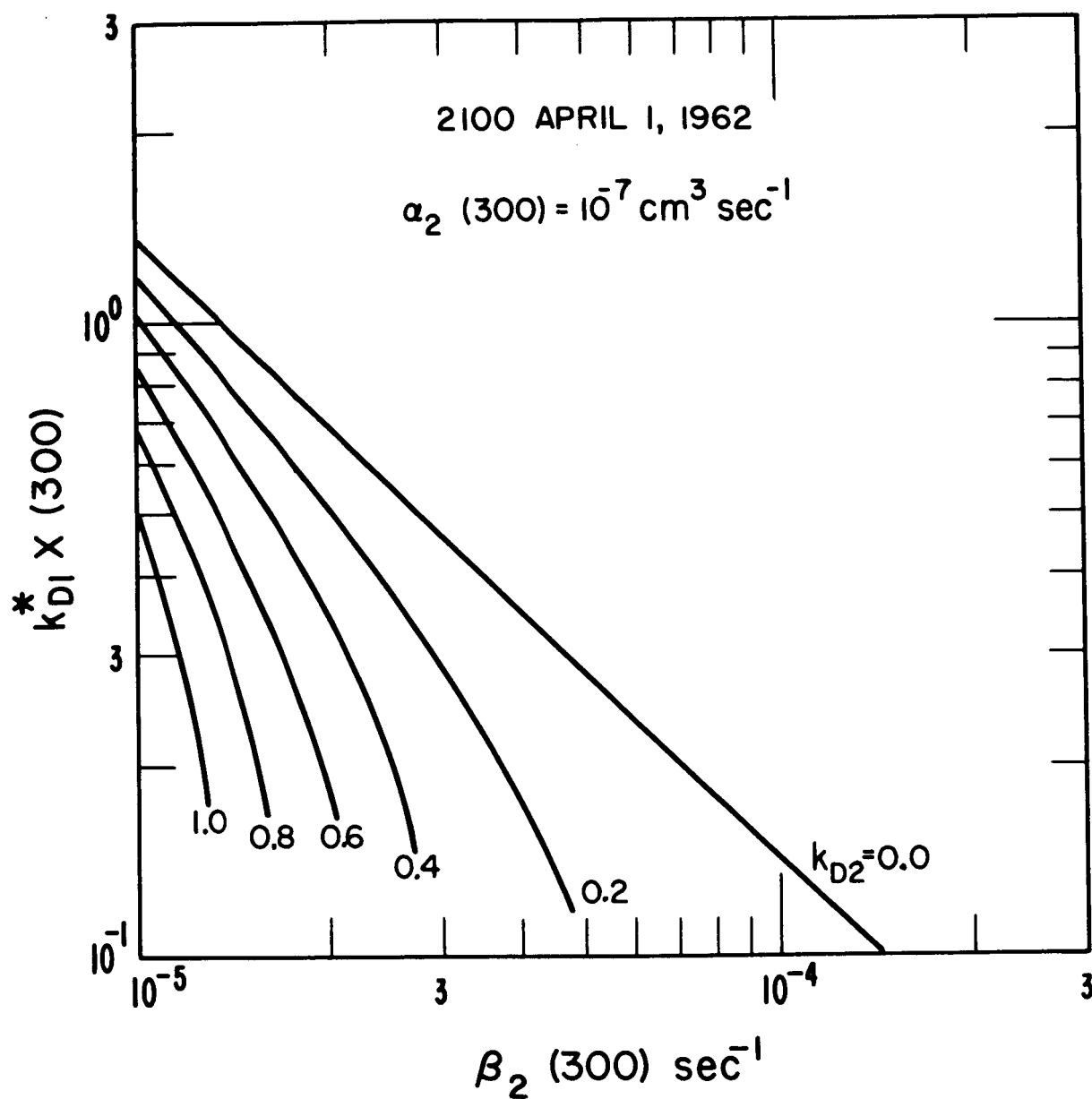


Figure 5. Combinations of k_{D2} , $\beta_2(300)$, and $k_{D1}^* X(300)$, for $\alpha_2(300) = 10^{-7} \text{ cm}^3 \text{ sec}^{-1}$, which give $Q(\text{calc}) = Q(\text{obs}) - Q(\text{back})$ for 2100 April 1, 1962.

The product $K(300) \beta_2(300)$ is sometimes found to vary during the period of observation, and sometimes found to be nearly constant. Figure 6 summarizes the results. Because the product is not completely independent of $\beta_2(300)$ (it varies by 10 to 20 percent as $\beta_2(300)$ is allowed to vary by an order of magnitude), the number given for the product in this figure is for $k_{D2} = 0$ and $k_{D1}^* X(300) = 0.1$ (these numbers were picked for reasons evident below). The time variations of the product do not seem unreasonable at the present state of our knowledge of the upper atmosphere.

The product $K(300) \beta_2(300)$ is generally between $\sim 10^{-5}$ and $\sim 5 \times 10^{-5} \text{ sec}^{-1}$, with a few excursions beyond these limits. Recent laboratory measurements [Fehsenfeld, et al., 1965] show that $\beta_2/[N_2] = \gamma_2 \approx 3 \times 10^{-12} \text{ cm}^3 \text{ sec}^{-1}$. Since model atmospheres normally give an N_2 number density at 300 km of 1 to $3 \times 10^8 \text{ cm}^{-3}$, the value of $\beta_2(300)$ would lie in the 3 to $9 \times 10^{-4} \text{ sec}^{-1}$ range. Thus $K(300)$ must be small, on the order of 0.1 or less. Dalgarno and Walker [1964] have pointed out that $k_{D2} \approx 0$; the present study shows that $k_{D1}^* X(300)$ is probably also small, about 0.1 or less. In other words, the efficiencies of the chemical reactions (discussed in Paper I) in producing $O(^1D)$ must be low.

Before discussing errors it must be pointed out that the present analysis has been for low latitude data; the quality 1 and 2 data show that the agreement between theory and observation is good. A similar but less detailed analysis of Fritz Peak - Boulder data [Peterson, unpublished] shows that at times theory and observation do not agree, whereas at other times they do agree; Fritz Peak - Boulder is, of course, mid-latitude.

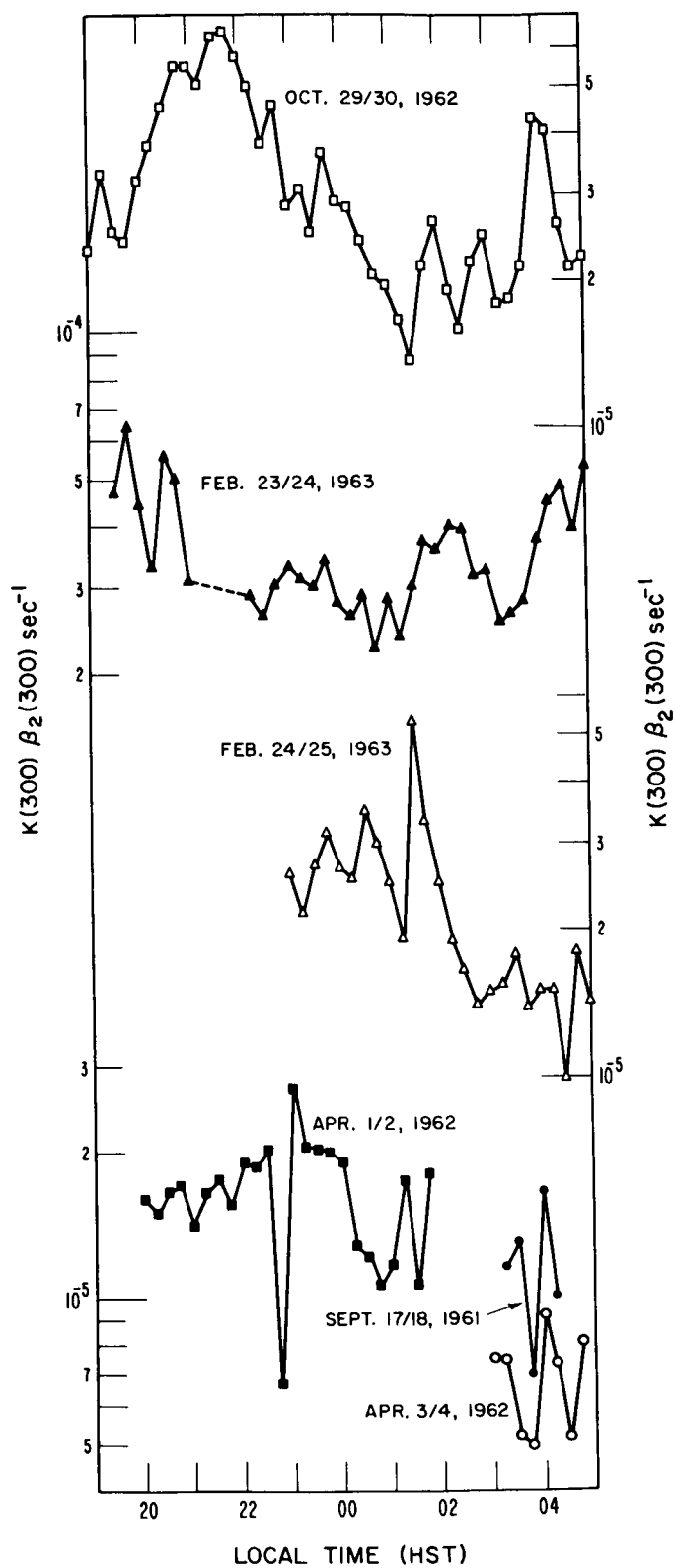


Figure 6. The values of $K(300) \beta_2(300)$ that give $Q(\text{calc}) = Q(\text{obs}) - Q(\text{back})$; as a function of time (Hawaiian Standard Time). The particular values plotted here are for $k_{D2} = 0$ and $k_{D1}^* X(300) = 0.1$, but these ordinate values differ little from those found by using other values of k_{D2} and $k_{D1}^* X(300)$. Note the staggered ordinate scale for the different curves.

ERRORS

The values of the product $K(300) \beta_2(300)$ quoted above are, of course, subject to various types of error. We shall now attempt to evaluate these errors and see what uncertainty this places on the estimate of this product.

The airglow observations are subject to error in three ways: in calibration, in record reading, and in contamination by extraneous light sources. The calibration errors (accuracy) are felt to be better than 50 percent. Because the relation between Q and $K(300) \beta_2(300)$ is nearly linear, the uncertainty in the product due to calibration errors is therefore also 50 percent or better. (In this paper, intensities have been calculated for the 6300Å emission line only and the 6364Å emission, which originates from the same level has been ignored. The observed intensities used, however, include the 6364Å contribution. Since this contribution (about 24 percent of the total) lies within the experimental uncertainties, its omission (an oversight of the authors) will not alter any of the conclusions of this paper.) The errors in reading the records (precision) are about 5 to 10 Rayleighs. Because this error is independent of the magnitude of the reading, it is meaningless to express it as a percent, unless the magnitude is also expressed. The error in $K(300) \beta_2(300)$ caused by reading imprecision will therefore be large for small Q , and small for large Q , the percent error in the product being about the same as the percent error in Q .

The errors introduced by the extraneous light that enters the photometer are difficult to estimate. Integrated starlight, zodiacal light, and continuum airglow are at least partially corrected for during data reduction, the estimated uncertainty in this correction being 5

Rayleighs. Occasionally a bright star will pass through the field of view and cause a large error in the reading, but these cases are easily identified and eliminated. The most uncertain contamination to the airglow data is that due to OH band emissions, specifically the OH(9-3) band with bandhead near 6256\AA . Based on data given by Chamberlain [1961], the OH contribution through the 6300\AA filter is estimated to be 10 to 20 Rayleighs, although it may be either larger or smaller than this and may even vary with time. The background component, $Q(\text{back})$, discussed in the preceding section is at least partially explained as being contamination by the above mentioned sources. As long as the contamination light remains fairly constant with time, as the data seem to indicate, no error will be introduced by this in the evaluation of $K(300) \beta_2(300)$.

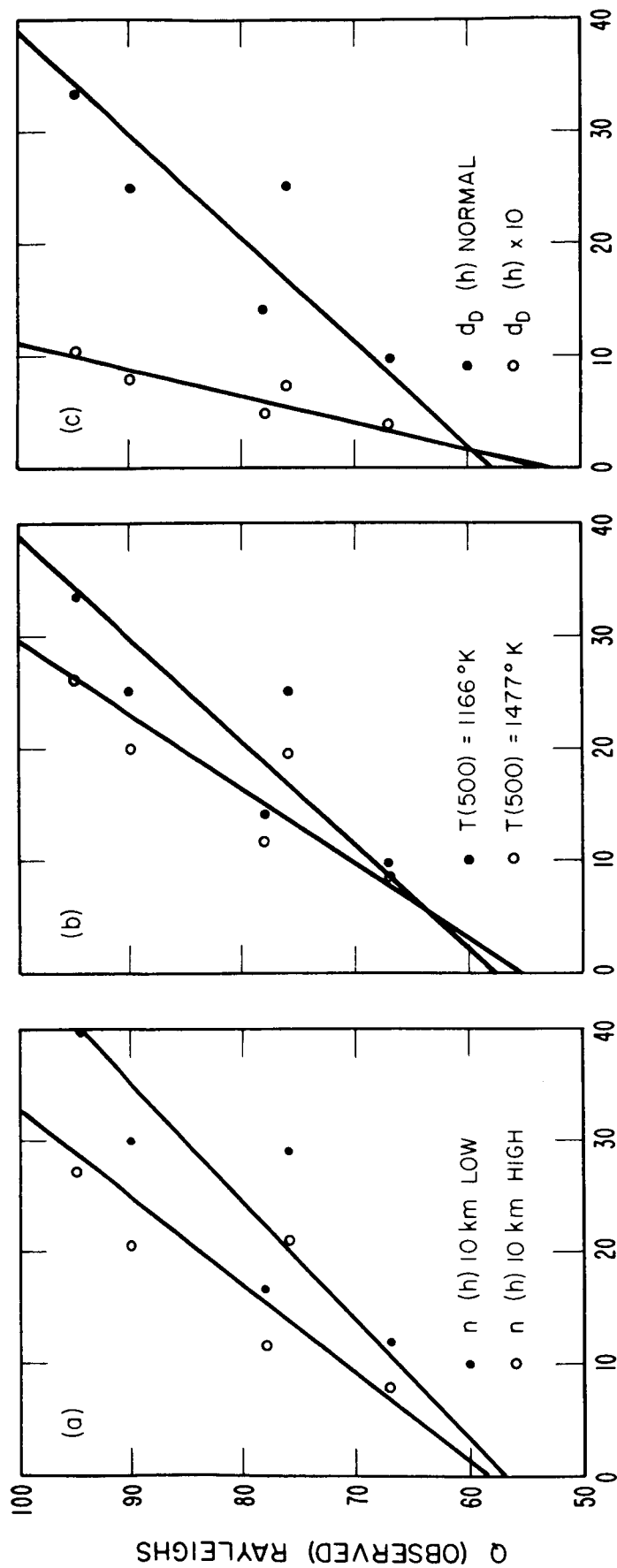
The $n(h)$ profiles are subject to errors in the ionogram reduction technique, to errors in the model "topside" used, and to errors caused by non-vertical radio echoes from the ionosphere. As mentioned above, the $n(h)$ profile deduced from an ionogram is sensitive to the detection of low-lying (E region) ionization; this was, as explained, the basis for breaking the data into different quality groups. The quality 1 data is felt to have an uncertainty in the true heights of about 5 to 10 km in the E region and of about 10 to 20 km in the lower F region, with the accuracy improving to about 5 to 10 km near the F region peak. The quality 2 data has about the same uncertainty as quality 1 for the F region, but for the E region the uncertainty is 20 to 40 km. The quality 3 data has an uncertainty of perhaps 50 km in the E and lower F regions, improving to about 10 to 20 km at the F region peak. Height errors at the peak will be carried over into the topside that is added on to the bottomside.

To evaluate the importance of such height errors, a series of $n(h)$ profiles were arbitrarily raised and lowered by 10 km; the product $K(300)$ $f_2(300)$ was found to change by about 15 percent for these cases, as shown in figure 7a. The height uncertainties in the quality 1 and 2 data, then, probably do not cause as much as a 15 percent uncertainty in this product. The height uncertainties in the quality 3 data, however, may cause about a 30 percent uncertainty in this product. It is important to note that height errors in $n(h)$ do not change the value of $Q(\text{back})$ deduced.

Errors in the topside model used are unimportant. For example, changing the scale height in the topside from 25 to 50 km, or from 50 to 100 km causes Q to change by only about 3 percent. Changing the scale-height gradient from 0 to 0.2 changes Q by less than 1 percent. Therefore, we may ignore errors in the topside model used.

Horizontal structure in the ionosphere can cause appreciable errors in the $n(h)$ profile deduced from the ionogram; if the radio echo returned to the ionosonde comes from several degrees away from the zenith, the deduced $n(h)$ profile may be either higher or lower than it should be. Since the horizontal structure is usually not known, there is no way to correct for these errors; however, the ionogram normally does reveal when such structure is present and so the user can know when to be wary. Fortunately, severe horizontal structure is not common over Maui and most of the data used in the present study are free of it.

The airglow and $n(h)$ errors discussed above produce a certain scatter of points in the graphs of $Q(\text{calc})$ vs $Q(\text{obs})$. This in turn causes an uncertainty in $Q(\text{back})$, which has precisely the same effect on $K(300)$



Q (CALCULATED) RAYLEIGHS

Figure 7. Comparison of the calculated and observed 6300Å nightglow intensities for Sept. 17/18, 1961, showing the effect of various types of error in the analysis. In (a), shifting the entire $n(h)$ profile up or down by 10 km changes the slope of the line, but changes $Q(\text{back})$ by only 1 or 2 Rayleighs. In (b), changing the temperature profile used again changes the slope of the line, but changes $Q(\text{back})$ by only about 2 Rayleighs. In (c), increasing the collisional deactivation profile by a factor 10 changes the line slope considerably but changes $Q(\text{back})$ by only about 5 Rayleighs. A change in the line slope indicates a corresponding change in $K(300) \beta_2(300)$. All lines shown have been calculated by the method of least squares.

$\beta_2(300)$ as does the lack of precision in reading the records, that is, the effect is larger for small Q than for large. The estimated uncertainty in $Q(\text{back})$ is indicated in table 2.

The temperature profiles used in this study were taken from the time varying model atmospheres of Harris and Priester [1962]. The night-time temperatures at 500 km in these models (for a 10.7 cm solar flux of 200 units) vary from 1166° to 1477°K. Since other model atmospheres have temperatures at 500 km ranging from 700° to 2000°K, it is important to know the effect of using the wrong temperature profile. By increasing $T(500)$ by 27 percent from 1166°K to 1477°K, Q is found to decrease by 25 percent as shown in figure 7b. Since the $T(500)$ values used for the present study are probably correct to within a factor of 2, the corresponding uncertainty in $K(300)$ $\beta_2(300)$ is probably also within a factor of 2. Again, it should be noted that errors in the choice of temperature profile do not change the value of $Q(\text{back})$ deduced, to any significant degree.

Finally, there is a large uncertainty in the collisional deactivation rate of $O(^1D)$. The $d_D(h)$ profile used was $d_D = s_D [O_2]$ with $s_D = 2 \times 10^{-11} \text{ cm}^3 \text{ sec}^{-1}$ and the $[O_2]$ from the 2300 model atmosphere of Harris and Priester [1962] for a 2800 Mc/s solar flux of 200 units. No time variations of $d_D(h)$ were allowed since s_D and $[O_2]$ are so poorly known. Wallace and Chamberlain [1959] have estimated that $4 \times 10^{-12} < s_D < 10^{-10} \text{ cm}^3 \text{ sec}^{-1}$; however, recent measurements of the dayglow [Wallace and Nidey, 1964; Dalgarno and Walker, 1964; Zipf, 1965] indicate that s_D is probably more on the order of $10^{-10} \text{ cm}^3 \text{ sec}^{-1}$. Thus, the values of $d_D(h)$ used in

the present study may be in error by as much as a factor of five or ten. To judge the effect of such an error on $K(300) \beta_2(300)$, the calculations were repeated for one night of data using $d_p(h)$ both increased and decreased by a factor of 10. The effect on $K(300) \beta_2(300)$ is significant: decreasing $d_p(h)$ by a factor of 10 decreases the product by about a factor of 2, whereas increasing $d_p(h)$ by a factor of 10 increases the product by about a factor of 3. The latter is shown in figure 7c. Again, however, it should be noted that an error in the choice of deactivation profile does not change the value of $Q(\text{back})$ deduced, to any significant degree.

By combining these uncertainties, the final uncertainty in the value of $K(300) \beta_2(300)$ can be estimated. We need consider only the uncertainties in $d(h)$ and $T(h)$ since these are so much larger than those in Q and $n(h)$. If the uncertainties in $d(h)$ and $T(h)$ combine unfavorably, $K(300) \beta_2(300)$ will be uncertain by about a factor of 4. However, it is likely that we have underestimated $d_p(h)$ and overestimated $T(h)$; these errors tend to cancel each other, leaving us with an uncertainty in $K(300) \beta_2(300)$ of about a factor of 2.

The possibility of observational bias cannot be entirely excluded. For example, it is possible that the desiderata for selecting ionograms excludes cases in which the theory does not work. However, since the nature of such an effect is unknown, there is no way to account for it.

SUMMARY

By applying the theory given in Paper I to an analysis of nightglow and $n(h)$ data, we draw three main conclusions. First, the theory does explain the observed variations in the 6300Å^o nightglow as being due to

corresponding changes in the height, shape, and magnitude of the electron density profile, at least for low latitude data. Second, the 6300Å night-glow that is recorded by the photometer is composed of two components: one component results from the chemical reactions discussed in Paper I and varies during the night. The other component seems to be independent of the chemical reactions discussed in Paper I and does not seem to vary much during any one night but may vary considerably from one night to another. The magnitude deduced for this second component is very insensitive to errors in the many parameters that enter the calculations. This background component is at least partially caused by contaminating light entering the photometer. Third, by subtracting out the background component, the "primary" component can be used to obtain an estimate of the product $K(300) \beta_2(300)$. The value of this product may vary during the night but generally it is between 10^{-5} and $5 \times 10^{-5} \text{ sec}^{-1}$. This estimate is probably correct to within a factor of 2. Because $\beta_2(300)$ is probably greater than 10^{-4} sec^{-1} , $K(300)$ must be on the order of 0.1; that is, the efficiency of the chemical reactions in producing $O(^1D)$ is low.

ACKNOWLEDGMENT

We are most grateful to J. W. Wright and his co-workers for reducing the ionograms to $n(h)$ profiles and for several enlightening discussions concerning the reliability of such calculations. This work was supported in part by NASA Grant #NsG-135-61.

REFERENCES

- Barbier, D., Recherches sur la raie 6300 de la luminescence atmospherique nocturne, Ann Geophys., 15, 179-217, 1959.
- Chamberlain, J. W., Oxygen red lines in the airglow. I. Twilight and night excitation processes, Astrophys. J., 127, 54-66, 1958.
- Chamberlain, J. W., Physics of the Aurora and Airglow, Academic Press, New York and London, 1961.
- Dalgarno, A. and J. C. G. Walker, The red line of atomic oxygen in the day airglow, J. Atmospheric Sci., 21, 463-474, 1964.
- Fehsenfeld, F. C., P. D. Goldan, A. L. Schmeltekopf, and E. E. Ferguson, Laboratory measurement of the rate of the reaction $O^+ + O_2 \rightarrow O_2^+ + O$ at thermal energy, Planetary Space Sci., 13, 579-582, 1965.
- Harris, I., and W. Priester, Time-dependent structure of the upper atmosphere, NASA Tech. Note D-1443, July 1962. Also J. Atmospheric Sci. 19, 286-301, 1962 (with abbreviated tables).
- Holmes, J. C., C. Y. Johnson, and J. M. Young, Ionospheric Chemistry, Space Research, V, North Holland Publishing Company, 756-766, 1965.
- Johnson, C. Y., E. B. Meadows, and J. C. Holmes, Ion composition of the arctic ionosphere, J. Geophys. Res., 63, 443-444, 1958.
- Lagos, P., W. Bellew, and S. M. Silverman, The airglow 6300A [OI] emission theoretical considerations on the luminosity profile, J. Atmospheric Terrest. Phys., 25, 581-587, 1963.
- Paul, A. K., and J. W. Wright, Some results of a new method for obtaining ionospheric N(h) profiles and their bearing on the structure of the lower F-region, J. Geophys. Res., 68, 5413-5420, 1963.

- Peterson, V. L., T. E. VanZandt, and R. B. Norton, F-region nightglow emissions of atomic oxygen I. Theoretical considerations, J. Geophys. Res., submitted 1965 (Paper I).
- Purdy, C. M., L. R. Megill, and F. E. Roach, A new airglow photometer, J. Res. NBS, 65C (Eng. and Instr.), No. 4, 213-216, October-December, 1961.
- Taylor, H. A., Jr., and H. C. Brinton, Atmospheric ion composition measured above Wallops Island, Virginia, J. Geophys. Res., 66, 2587-2588, 1961.
- Wallace, L., and J. W. Chamberlain, Excitation of O₂ atmospheric bands in the aurora, Planetary Space Sci., 2, 60-70, 1959.
- Wallace, L., and R. A. Nidey, Measurement of the daytime airglow in the visual region, J. Geophys. Res., 69, 471-479, 1964.
- Zipf, E. C., Jr., Rocket measurement of the visual dayglow, J. Geomag. Geoelec., in press, 1965.